A Simple Cross Correlation Switched Beam System (XSBS) for Angle of Arrival Estimation

IEEE Access
Multidisciplinary | Rapid Review | Open Access Journal

Received January 23, 2017, accepted February 10, 2017, date of publication February 14, 2017, date of current version March 28, 2017.

Digital Object Identifier 10.1109/ACCESS.2017.2669202

A Simple Cross Correlation Switched Beam System (XSBS) for Angle of Arrival Estimation

AHMED BADAWY[1], (Student Member, IEEE), TAMER KHATTAB[2], (Member, IEEE), DANIELE TRINCHERO[1], (Member, IEEE), TAREK M. ELFOULY[3], (Senior Member, IEEE), AND AMR MOHAMED[3] (Member, IEEE)

[1]Department of Electronics and Telecommunication, Politecnico di Torino, 10129 Torino, Italy
[2]Department of Electrical engineering, Qatar University, Doha 2713, Qatar
[3]Department of Computer science and Engineering, Qatar University, Doha 2713, Qatar

Corresponding author: A. Badawy (ahmed.badawy@polito.it)

This work was supported of the National Priorities Research Program Grant 5- 559-2-227 from the Qatar National Research Fund.

ABSTRACT We propose a practical, simple and hardware friendly, yet novel and efficient, angle of arrival (AoA) estimation system. Our intuitive, two-phases cross-correlation-based system requires a switched beam antenna array with a single radio frequency circuitry, which is used to collect an omni-directional reference signal using a single element of the antenna array in the first phase. Our system applies energy detection on the collected reference signal to decide on the presence or absence of a transmitted signal. In the second phase, the system steers the main beam to scan the angular region of interest. The collected signal from each beam angle is cross correlated with the omni-directional reference signal to determine the angle of arrival of the received signal. The combined practicality and high efficiency of our system is demonstrated through performance and complexity comparisons with one of the literature's best performing multiple signal classification (MUSIC) algorithm. Our proposed AoA estimation system has a negligible root mean square error at signal to noise ratio level greater than -16 dB, which is very comparable to MUSIC.

INDEX TERMS Angle of arrival estimation, AoA, direction of arrival estimation, switched beam, cross correlation.

I. INTRODUCTION

Angle of arrival (AoA) estimation is a process that determines the direction of arrival of a received signal by processing the signal impinging on an antenna array. Estimating the AoA is a crucial step in many military and civilian applications, particularly related to security. Applications of estimating the AoA include beamforming, tracking [1], localization and physical layer secrecy [2].

The subject of AoA has been extensively studied in the literature [3]–[7]. From a system perspective, one can categorize AoA estimation systems into two main categories [3]: **(i) Switched beam system (SBS)** which uses a fixed number of beams to scan the azimuth plane. The AoA is the angle of the beam with the highest received signal strength (RSS). SBS is easy to implement since it requires a single receiver radio frequency (RF) chain and no baseband signal processing, however, it fails at low signal to noise ratio (SNR) levels, and **(ii) Adaptive array system (AAS)** which can steer the beam in any desired direction using baseband signal processing. AAS requires M receiver RF chains to estimate the AoA using baseband processing, where M is the number of antennas. AAS can operate at SNRs lower than SBS, but has higher hardware and computational complexities.

AoA estimation using AAS can be divided into two main techniques: **(1) Classical AoA techniques** based on one of two main methods: *Delay and Sum*, also known as *Bartlett* [8] and *Minimum Variance Distortionless Response (MVDR)*, also known as *Capon* [9]. In Bartlett, the AoA is estimated by steering the beams electronically and estimating the power spectrum of the received signal looking for the angle(s) corresponding to peak(s) in the spatial power spectrum. The main drawback of the Bartlett technique is that signal impinging with angular separation less than $2\pi/M$ can not be resolved. The Capon technique relatively solves the angular resolution drawback of the Bartlett method at the cost of more baseband processing to perform matrix inversion [9], and **(2) Subspace techniques** based on the concept of orthogonality of signal subspace to noise subspace. The most widely investigated method in this group is multiple signal classification (MUSIC) [10], [11], which was developed in 1981.

MUSIC provides high angular resolution while operating at low SNR levels as well as performance close to the Cramer Rao bound. This comes at the cost of requiring full a priori knowledge of the number of sources and the array response, whether measured and stored or computed analytically [12]. The signal and noise subspaces are distinguished through an eigen decomposition operation on the covariance matrix of the received signal. This operation requires a substantial computational complexity. Another technique that is subspace based is the Estimation of Signal Parameters via Rotational Invariant Technique (ESPRIT) [13], [14], which was developed in 1989. Although ESPRIT has lower computational complexity relative to MUSIC technique since it does not require a sweeping through all possible array response and does not require the signals to be uncoherent as in MUSIC, it puts a constraint on the structure of the antenna array. ESPRIT requires that the antenna element to be clustered in doublet with identical displacement vector. The performance of MUSIC is slightly better than ESPRIT [15].

Recent publications [16], [17] exploit the newly developed concept of co-prime arrays to estimate the AoA. In addition, Kalman filtering is used in [18] in the first stage to estimate the sources, while QR decomposition is needed in the second stage to estimate the AoA. Although Kalman filter based techniques may have lower computational complexity than MUSIC, they have high computational and hardware complexity when compared to SBS.

Due to its attractive simplicity, several attempts have been performed to integrate SBS with other theories to estimate the AoA as presented in [19]. Their methodology is based on neural network, in which the AoA problem is transferred into a mapping problem. This requires a priori knowledge of the number of sources as well as the multiple access scheme adopted between them. It is also assumed that a power control scheme is implemented such that the source powers are equal. Such requirements and assumptions limit the deployment of the system to very few scenarios. Exploiting the power ratio between adjacent beams to estimate the AoA is presented in [20]. A table driven SBS system is presented in [21], which requires a pilot signal to be sent first, which is not applicable in our system as well as MUSIC or ESPRIT. It already assumes that the transmitter is collaborating with the receiver, which is not a typical assumption in any of these techniques. All of these variant techniques do not tackle the drawbacks of the conventional SBS, but rather make its implementation easier. In addition, [22] exploit sectorized antennas to improve the performance of SBS.

The concept of using the cross-correlation function to extract features of a signal, or to detect its presence, can be found in many applications. One of the most relevant applications is passive radar systems [23], [24], which exploit the transmitters of opportunity, such as television signals, to detect an airborne target. In passive radar systems, a cross correlation between a reference signal from the first receiver and a directional signal from the second is applied to estimate bistatic range and doppler shift of the target. The AoA has to be estimated before that at the second receiver to place a null in the direction of the reference signal [23], [24] such that the received directional signal is the reflection from the airborne target. Another relevant application is localization, in which a cross correlation between two signals received from two antennas is applied to estimate the time difference of arrival [25]–[27].

Direct applications of AoA estimations systems is estimating the AoA of a cooperating transmitter in order to direct the main beam in its direction so as to increase the SNR and hence increase the transmission rate. On the other hand, in a battlefield, an enemy will try to hide its transmitted signal such that his location cannot be detected. In addition, a jammer will try to hide by transmitting the jamming signal at different times from different locations. In these two examples, it is crucial to locate the adversarial transmitters, in which AoA estimation is a necessary step. In the case of mobile sensor units deployed in rural areas, the sensor nodes will only send data, for example a rescue call, whenever they are available. In this case, the source node will transmit at random times, which in this case considered an unintentional hiding.

In this paper, we propose a new simple AoA estimation system. Our system goes through two phases of operation. In the first phase, we listen to the frequency spectrum of interest and apply a sensing technique, namely energy detection (ED), to decide on the presence or absence of the transmitted signal. The transmitter is transmitting at random times, therefore, applying AoA estimation technique at all times will consume extensive processing and power. Applying spectrum sensing technique a priori will allow us to efficiently minimize the processing burden and minimize the consumed power, which is extremely useful, particularly, in case of portable receivers. In this phase, we select a single antenna element from the antenna array, while the rest of antenna elements are switched off, to collect an omni-directional signal for the spectrum sensing technique. Once the presence of the transmitted signal is detected, the system switches to the second phase which is AoA estimation. In the second phase our system switches the beam across the azimuth angular domain of interest. The received signal from each beam is then cross correlated with the omni-directional signal collected earlier in the first phase for the purpose of sensing the spectrum. The cross correlation between the omni-directional signal and the signals received from the switched beams is the highest at the true AoA and relatively negligible otherwise. Our contributions in this work as compared to available literature are as follows:

- We propose an intuitive, novel, low complexity and hardware friendly two-phase cross correlation based AoA estimation system that is based on SBS.
- We provide the mathematical modelling and analysis of our proposed system.
- We address some practical aspects related to our proposed system.
- We compare the performance of the proposed system with the MUSIC algorithm (famous for being one of

the best performing state-of-the-art for low SNR) and show that our proposed solution has a comparable performance to MUSIC.
- We also compare the computational complexity of our approach with MUSIC and conclude that our approach has lower hardware and computational complexities.

Since our system is based on beam switching, it requires a single receiver which reduces the hardware complexity tremendously. Also, the computational complexity of estimating the cross correlation coefficient is so trivial when compared to estimating the eigen decomposition of the auto-covariance function used in MUSIC. To the best of the authors' knowledge using the cross correlation coefficient between an omni-directional signal and directed beam signal to estimate the AoA has not been presented in the literature before.

The notation throughout the paper is chosen as: unbold letters to represent single samples, small bold letters to represent vectors and capital bold letters to represent matrices.

The rest of this paper is organized as follows: In Section II our system model is presented. A review of MUSIC algorithm is presented in Section III. We then propose our two-phase cross correlation based AoA estimation system in Section IV. Practical aspects of our system are addressed in Section V. The performance of our proposed system is evaluated in Section VI. Analysis of the complexity of our AoA estimation method is provided in Section VII. The paper is concluded in section VIII.

II. SYSTEM MODEL

In our system model, we assume that there exists a transmitter, whether it is a cooperating or adversarial transmitter that is transmitting a signal $s(t)$ at random times with random power. Our receiver is equipped with an SBS, presented in Figure 1, consisting of M antenna elements, separated by a fixed separation d and operating at frequency f. Our antenna array has an array response vector (steering vector) $\mathbf{a}(\phi) \in \mathbb{C}^M$ given by

$$\mathbf{a}(\phi_k) = [w_{k1}, w_{k2}, \ldots, w_{kM}], \tag{1}$$

where ϕ is the azimuth angle, $\mathbb{C}$ is the set of complex numbers and w_{km} for $m \in [1 : M]$ are the weights applied across the antenna array elements such that the steering vector $\mathbf{a}(\phi)$ is pointing to an azimuth angle ϕ_k. The received and sampled signal, $x[n]$, in the vector notation for the k^{th} beam, $\mathbf{x_k}$, is

$$\mathbf{x_k} = \mathbf{a}(\phi_k)\mathbf{S} + \mathbf{v}, \tag{2}$$

where $\mathbf{x_k}$ (with dimensions $1 \times N$) is the signal received from the k^{th} beam (beam pointing at angle ϕ_k) for $k \in [1 : K]$, K is the total number of generated beams, N is the total number of collected samples, $\mathbf{S}$ is the sampled version of the transmitted signal (with dimensions $M \times N$) as seen by the M elements of the antenna array and $\mathbf{v}$ is the additive white Gaussian noise (AWGN) (with dimensions $1 \times N$). The number of sources, i.e., the number of AoAs, is denoted by L.

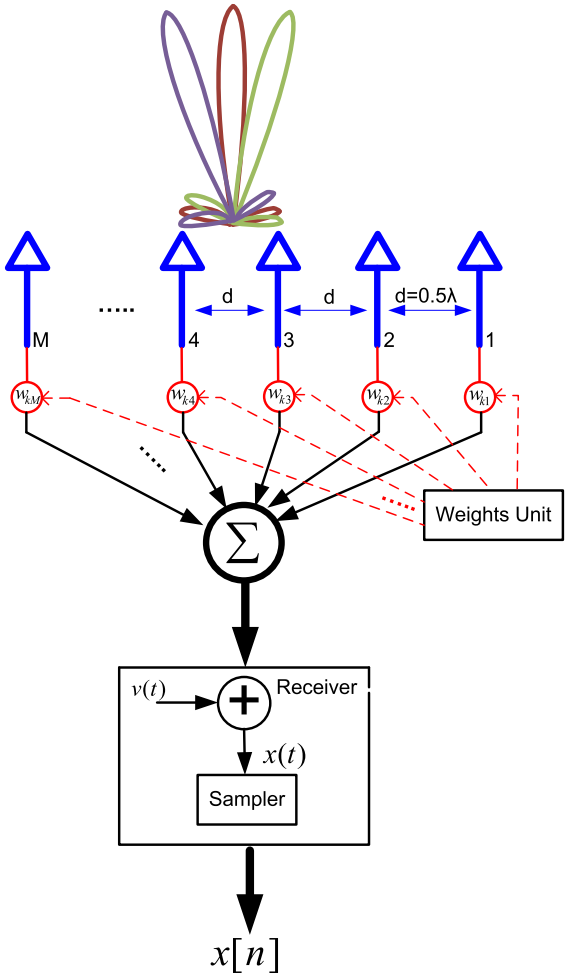

FIGURE 1. Proposed cross correlation switched beam system for *M* antenna elements.

The weights are updated to change ϕ_k in order to scan the angular space of interest. The steering vectors, $\mathbf{a}(\phi)$, for linear, circular or planar array formations can be calculated analytically. It is worth noting that once the steering vector is set, the operation of our proposed system is independent of the antenna array formation. For a uniform linear array (ULA) with uniform excitation, $\mathbf{a}(\phi)$ is given by [3]:

$$\mathbf{a}(\phi) = \left[1, e^{j\beta dcos(\phi)}, e^{j\beta 2dcos(\phi)}, \ldots, e^{j\beta(M-1)dcos(\phi)}\right], \tag{3}$$

where $\beta = \frac{2\pi}{\lambda}$ is the wave number, λ is the wavelength and ϕ ranges between $[0 : \pi]$. For a uniform circular array (UCA), $\mathbf{a}(\phi)$, is given by [3]:

$$\mathbf{a}(\phi) = [e^{j\beta r\cos(\phi-\phi_1)}, e^{j\beta r\cos(\phi-\phi_2)}, \ldots, e^{j\beta r\cos(\phi-\phi_M)}], \tag{4}$$

where $\phi_m = 2\pi m/M, m \in [1 : M]$, ϕ ranges between $[0 : 2\pi]$ and r is the radius of the antenna array. To steer the main beam of the antenna array towards a desired angle ϕ_k, i.e., obtain $\mathbf{a}(\phi_k)$, substitute $\phi = \phi_k$ in (3) or (4). The elevation angle is assumed to be 90 degrees in 1-D AoA

estimation techniques. For a linear array of M elements with uniform excitation, the total number of orthogonal beams that can be generated is M, i.e., $K = M$. However, using non-uniform excitation such as Dolph-Chebyshev or Taylor [28], it is possible to generate more orthogonal beams for the same number of antenna elements, M, i.e., $K > M$, as will be discussed later.

We assume that the our scanning time is much less than the time it takes the transmitter to move from one location to the next. In addition, we assume that the transmitter continues to transmit highly correlated signal during our scanning time. This can be safely assumed since the scanning time should not exceed few milliseconds.

III. REVIEW OF MUSIC ALGORITHM

Since we compare our results to the MUSIC algorithm, a brief derivation follows for completeness. We chose to compare our results to MUSIC for two main reasons. The first is that MUSIC is one of literature's best performing AoA estimation algorithms [15], [29]. In addition, MUSIC is one of the most popular AoA estimation algorithms. MUSIC requires M receiver RF chains to down convert the received signals from the M antenna elements to the baseband in order to estimate the AoA. Hence, the definition and dimensions of the transmitted signal matrix is different than our SBS system above. The received signal, $\mathbf{X}$, is a matrix with dimensions $M \times N$. The MUSIC algorithm operates on the autocovariance function of the received signal matrix $\mathbf{X}$, with dimensions $M \times N$, which is denoted by $\mathbf{R}_{XX}$. Let $\mathbf{A} = [\mathbf{a}^T(\phi_1), \cdots, \mathbf{a}^T(\phi_L)]$, with dimensions $M \times L$, and $(.)^T$ denotes the transpose operation. Also, let $\mathbf{s}(t) = [s_1(t), \cdots, s_L(t)]^T$. We have [29]

$$\mathbf{X} = \mathbf{AS} + \mathbf{V}, \tag{5}$$

where $\mathbf{S}$ and $\mathbf{V}$ have dimensions of $L \times N$ and $M \times N$, respectively. After an eigenvalue decomposition (EVD) on $\mathbf{R}_{XX}$, it can be written as [29]

$$\begin{aligned} \mathbf{R}_{XX} &= \mathbf{A}\mathbf{R}_{SS}\mathbf{A}^H + \sigma^2 I \\ &= U_S \Lambda_S U_S^H + U_V \Lambda_V U_V^H, \end{aligned} \tag{6}$$

where $\mathbf{R}_{SS}$ is the autocovariance matrix of the transmitted signal, σ^2 is the noise variance, $(.)^H$ denotes the hermitian operation, $\mathbf{I}$ is the $M \times M$ unitary matrix, $\mathbf{U}_S$ and $\mathbf{U}_V$ are the signal and noise subspaces unitary matrices and Λ_S and Λ_V are diagonal matrices of the eigenvalues of the signal and noise. The spatial power spectrum for the MUSIC technique is given by [10], [30]:

$$P_{\text{MUSIC}}(\phi) = \frac{1}{\mathbf{a}^H(\phi) P_V \mathbf{a}(\phi)}, \tag{7}$$

where $P_V = U_V U_V^H$. For MUSIC, number of sources is a prerequisite. If the number of sources is not known a priori, it should be estimated prior to AoA estimation and fed to MUSIC.

IV. PROPOSED CROSS-CORRELATION SWITCHED BEAM SYSTEM (XSBS)

The existing high performance AoA estimation techniques either have a low resolution problem or require extensive computational complexity to estimate the AoA. Moreover, they require M receivers to implement the AoA estimation technique which increases the hardware complexity tremendously. On the other hand, although conventional SBSs have low hardware and computational complexities, they fail to operate at medium and low SNR levels.

We propose a novel cross-correlation based SBS (XSBS) AoA estimation technique. Our XSBS benefits from the low hardware complexity of the conventional SBS, which requires a single receiver, yet does not sacrifice the resolution or performance at medium and low SNR levels. Moreover, our XSBS requires low computational complexity to estimate the AoA since it is based on estimating the cross correlation between two collected one dimensional vector of samples. With such low hardware and computational complexity, our XSBS will consume less power which will be very beneficial, particularly, if implemented on a portable device. Furthermore, XSBS requires neither prior information on the number of the sources nor the sources to be uncorrelated.

In the following, we provide a detailed description of the operation of our proposed XSBS alongside the corresponding basic mathematical modelling of the system.

A. XSBS DESIGN

XSBS goes through two phases to estimate the AoA as follows. A flow chart of our XSBS phases of operation is depicted in Fig. 2.

- **Phase I**: the *Weights Unit* depicted in Fig. 1 controls the RF switches such a single antenna element is turned on, while the remaining antenna elements are switched off. In the selected antenna element branch, the applied weight is unity gain and zero phase shift. Assuming approximate omni-directional pattern for individual antenna elements, XSBS then acquires N samples to collect the signal $\mathbf{x}_o$. The spectrum sensing technique is then applied on $\mathbf{x}_o$. The decision statistic $(T(\mathbf{x}_o))$ is compared to a threshold (γ_o) to decide on the presence or absence of the transmitted signal.
- **Phase II**: Once a detection of a transmitted signal is declared, our XSBS proceeds to the second phase. In this phase the omni-directional signal collected in the first phase, i.e., $\mathbf{x}_o$, becomes our reference signal. The *Weights Unit* sends the sets of weights $\mathbf{a}(\phi_k)$, for $k \in [1 : K]$. The set $\mathbf{a}(\phi_k)$ steers the main beam of the antenna array to the direction ϕ_k. XSBS then acquires N samples to collect the signal $\mathbf{x}_k$. A cross correlation operation between our reference signal $\mathbf{x}_o$ and the k^{th} beam signal is applied. The cross correlation coefficient (R_{ko}) is calculated for K beams. The AoA is the index $\hat{\phi}_k$ with the highest R_{ko}.

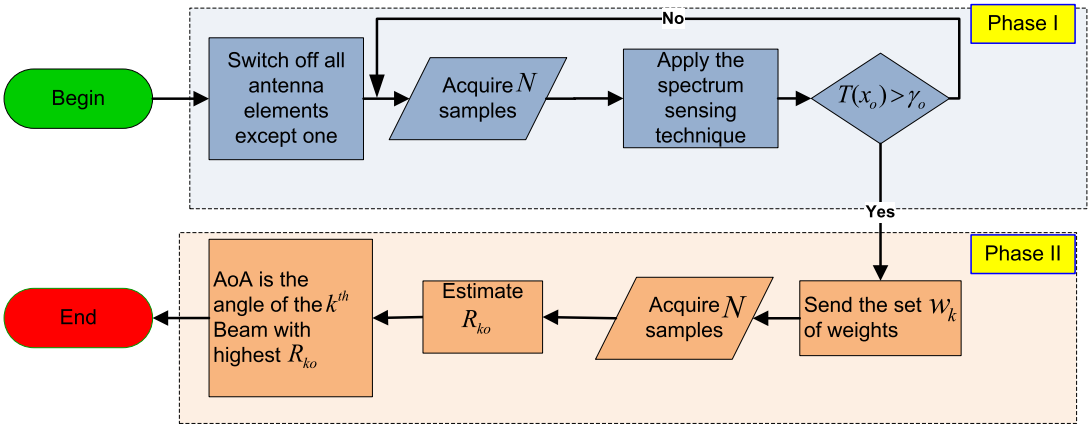

FIGURE 2. Flow chart of our proposed XSBS.

Applying a spectrum sensing technique enables XSBS to be power efficient since the AoA estimation in Phase II is only applied once a detection of the transmitter signal is confirmed. Therefore, the extra processing needed to estimate the AoA is only performed when needed. Due to its low cost implementation, we adopt energy detection as our XSBS spectrum sensing technique to decide on the presence or absence of the transmitted signal.

Note that if a front-end circuitry that improves the sensitivity is added only on the reference antenna branch, the performance of spectrum sensing operation and the overall XSBS system will improve. For linear antenna array, the reference antenna should be the one in the middle, however for a circular array, any antenna can be used as the reference.

B. SPECTRUM SENSING BASED ON ENERGY DETECTION

As XSBS is listening to the spectrum of interest in Phase I, it acquires N samples to collect the samples $x_o[n]$. There are two hypotheses within the detection of the transmitted signal, $s_m[n]$, framework:

$$H_0 : x_o[n] = v[n], \quad \text{for } n = 1, \cdots, N. \tag{8}$$

$$H_1 : x_o[n] = G_o s[n] + v[n], \quad \text{for } n = 1, \cdots, N. \tag{9}$$

where G_o is the omni-directional antenna element gain and H_0 and H_1 represent the statuses when the spectrum is empty and occupied by the transmitted signal, respectively. The decision statistic for the energy detection technique is given by [31]:

$$T(x_o) = \frac{1}{N} \sum_{n=1}^{N} |x[n]|^2 \underset{H_0}{\overset{H_1}{\gtrless}} \gamma_o. \tag{10}$$

The objective of transmitting the signal with random power is to hide it within noise. Hence, under hypothesis H_0, $\mathbf{x}_o$ follows $\mathcal{CN}(0, \sigma^2)$ and under hypothesis H_1, $\mathbf{x}_o$ follows $\mathcal{CN}(0, \sigma^2 + P)$[1], where P is the received power of the transmitted signal. XSBS does not require any prior information about the transmitted signal. The decision statistic in (10) is a summation of N squared Gaussian random variables. Hence, it follows Chi-Square distribution. The probability of false alarm, P_f is given by [32]:

$$P_f = Pr\{T(x_o) > \gamma_o | H_0\} = \frac{\Gamma(\frac{N}{2}, \frac{\gamma_o}{2\sigma^2})}{\Gamma(\frac{N}{2})}, \tag{11}$$

where $\Gamma(\cdot)$ is the Gamma function and $\Gamma(\cdot, \cdot)$ is the incomplete Gamma function. Hence for a desired p_f, the threshold, γ_o is estimated.

C. CROSS CORRELATION ESTIMATION

In the second phase of estimating the AoA, XSBS cross correlates the omni-directional reference signal, $\mathbf{x_o} = [x_o[1], \cdots, x_o[n], \cdots, x_o[N]]$, with the directed beam signals, $\mathbf{x_k} = [x_k[1], \cdots, x_k[n], \cdots, x_k[N]]$, for $k \in [1 : K]$ through the region of interest as in (2). $\mathbf{x_o}$ and $\mathbf{x_k}$ are pass-band signals. The cross correlation coefficient between the reference signal and the k^{th} signal is given by

$$R_{ko} = \frac{1}{N}\left(\mathbf{x_k}\, \mathbf{x_o^H}\right). \tag{12}$$

The cross correlation between the omni-directional reference signal and the signals received from the switched beams is the highest at the true AoA and relatively negligible otherwise. To show that, we provide the derivation below. The received signal from the k^{th} beam if k is the true AoA is

$$x_k^{Tr}[n] = G_k s[n + \tau] + v[n + \tau], \tag{13}$$

where G_k is the directive antenna array gain and τ is a random time shift. The received signal from the k^{th} beam if k is not the true AoA is $x_k^F[n] = v[n + \tau]$. The cross correlation function in the case of the true AoA, R_{ko}^{Tr}, can be written as

$$R_{ko}^{Tr} = \frac{1}{N} \sum_{n=1}^{N} x_k^{Tr}[n]\, x_o^H[n]$$

$$= \frac{1}{N} \sum_{n=1}^{N} \Big[(G_k\, s[n + \tau] + v[n + \tau])$$

[1] $\mathcal{CN}$ stands for complex normal distribution.

$$\times \left(G_o\, s^H[n] + v^H[n]\right)\Big]$$
$$= \frac{G_o G_k}{N}\sum_{n=1}^{N} s[n+\tau]\, s^H[n] + \frac{G_k}{N}\sum_{n=1}^{N} s[n+\tau]\, v^H[n] + \frac{G_o}{N}\sum_{n=1}^{N} v[n+\tau]\, s^H[n] + \frac{1}{N}\sum_{n=1}^{N} v[n+\tau]\, v^H[n]. \quad (14)$$

The cross correlation function in the case that k is not the true AoA, and assuming no signal is leaked from side lobes, R^F_{ko}, can be written as

$$R^F_{ko} = \frac{1}{N}\sum_{n=1}^{N} x^F_k[n] x^H_o[n] = \frac{1}{N}\sum_{n=1}^{N} (v[n+\tau])\left(G_o s^H[n] + v^H[n]\right) = \frac{G_o}{N}\sum_{n=1}^{N} v[n+\tau]\, s^H[n] + \frac{1}{N}\sum_{n=1}^{N} v[n+\tau]\, v^H[n]. \quad (15)$$

With R_{ss} being the autocorrelation function of $s[n]$, R_{sv} the cross correlation between $s[n]$ and $v[n]$, and $s[n]$ and $v[n]$ are stationary processes, (14) can be written as

$$R^{Tr}_{ko} = G_o G_k\, R_{ss}[\tau] + G_k\, R_{sv}[\tau] + G_o\, R_{vs}[\tau] + \sigma^2, \quad (16)$$

where σ^2 is the noise variance. (15) can be written as

$$R^F_{ko} = G_o R_{vs}[\tau] + \sigma^2. \quad (17)$$

Since $s(t)$ and $v(t)$ are uncorrelated, R_{sv} and R_{vs} can be considered negligible. Consequently, (16) and (17) reduce to:

$$R^{Tr}_{ko} = G_o G_k R_{ss}[\tau] + \sigma^2, \quad (18)$$
$$R^F_{ko} = \sigma^2. \quad (19)$$

From (18) and (19), one can see that $R^{Tr}_{ko} > R^F_{ko}$. As the transmitted power increases, $R^{Tr}_{ko} \gg R^F_{ko}$. For the case where there is a signal that is leaked from a side lobe, (19) can be rewritten as:

$$R^F_{ko} = \frac{G_o G_k}{R} R_{ss}[\tau] + \sigma^2, \quad (20)$$

where R is the main lobe to side lobe ratio, which is a design parameter. Hence for higher main lobe to ratio, the effect of signal leaked through side lobe is minimized. We propose binary search in Sec V-C to address this issue and we dedicate Sec VI-C3 to show the effect of R on the performance of XSBS.

V. ADDRESSING PRACTICAL ASPECTS

In this section, we address some practical aspects of our proposed XSBS. We start by presenting a schematic of XSBS, which details the required components needed to implement XSBS. Then, we proceed to discuss incorporating non-uniform excitation in order to increase the total number of orthogonal generated beams.

A. SCHEMATIC OF XSBS

Fig. 3 shows the proposed schematic of XSBS. Each antenna is connected to an RF switch, attenuator and phase shifter. Signals from all antenna branches are combined using an RF combiner/divider. A receiver circuitry is then followed to down-convert the collected signal into baseband in order to be processed by the digital signal processing (DSP) unit, which triggers the weights unit to send the pre-calculated weights to the attenuators and phase shifters in order to steer the main beam of the antenna array. The RF switches are added, primarily, because of Phase I of XSBS operation. During this phase, the omni-directional signal, $\mathbf{x_0}$, should be collected from a single antenna branch. RF switches are used to turn on the selected branch and turn off the unwanted ones. This minimizes the leaked signal from the unwanted branches, which could be leaked through the attenuators and phase shifters. During Phase II of XSBS operation, all the RF switches are turned on.

B. NUMBER OF GENERATED ORTHOGONAL BEAMS

Orthogonal beams indicate that the peak of the current beam is located at a minima of the two adjacent beams. Hence, when collecting a signal from one beam (assuming a signal is impinging from the direction of the peak), no signal is leaked from its adjacent ones. M is a key factor in determining the resolution of our XSBS. The higher the number of antenna elements, the smaller the half power beam width (HPBW) of the antenna array beam. Hence, our AoA location grid (assuming orthogonal beams) can become finer and finer, i.e., covering more and more locations as required. A smaller HPBW leads to a better resolution. It is possible to generate as many non-orthogonal beams as possible. For example, for ULA, it is possible to generate 180 beams. However, this approach will increase the scanning time significantly. When using orthogonal beams, the signal impinging on directions that are not the peak location, will be detected by two adjacent beams with different powers. We will show in Sec VI-C1, that by simply using weighted average, we can detect all AoAs with almost same accuracy. In weighted average the two adjacent peaks are compared and if for example, they are approximately equal, then the signal is impinging at a direction, which is the mid-angle between the two adjacent peaks. On the contrary, a higher M will increase the hardware complexity of XSBS since they will require more weight adjustment components.

Using a non-uniform excitation such as Dolph-Chebyshev excitation, it is possible to generate more *orthogonal* beams

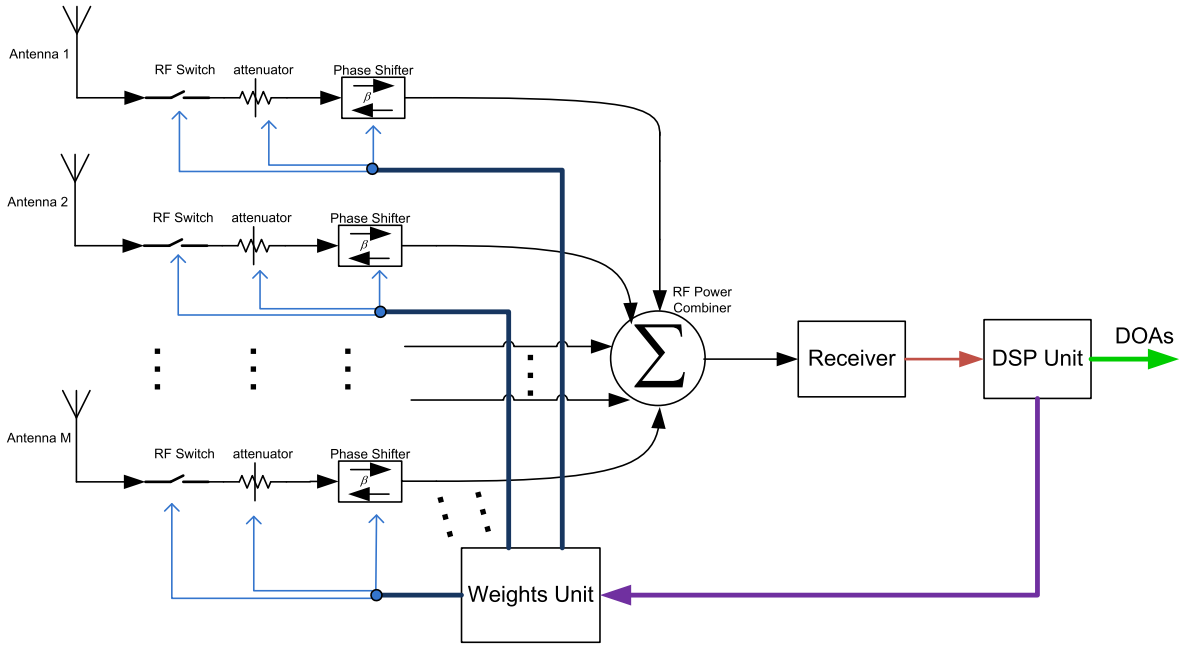

FIGURE 3. Schematic of proposed XSBS.

using the same M antenna elements. In this case, for ULA, the Dolph-Chebysehev array factor $\mathbf{w}(\psi)$ is defined by the Chebyshev polynomial of degree $M-1$, $\mathbf{t}_{M-1}(y)$, in the scaled variable y as [28]:

$$\mathbf{w}(\psi) = \mathbf{t}_{M-1}(y), \quad y = y_0 \cos\left(\frac{\psi}{2}\right). \tag{21}$$

We have $\psi = \beta d \cos(\phi)$ and the scale factor, y_0, is estimated as $y_0 = \cosh\left(\frac{\cosh^{-1}(R)}{M-1}\right)$, where $\cosh^{-1}(.)$ is the inverse hyperbolic cosine function, R is the main lobe to side lobe ratio. The elements of the Dolph-Chebysehev weight vector $\mathbf{a}_d(\phi_k)$ for a fixed k and $m \in [1 : M]$ can be calculated by creating the z-transform function of the array response factor from its zeros and then applying an inverse z-transform. The $M-1$ zeros of $\mathbf{t}_{M-1}(y)$ are [28]:

$$y_i = \cos\left(\frac{(i-1/2)\pi}{M-1}\right), \quad \text{for } i = 1, 2, \ldots, M-1. \tag{22}$$

The pattern zeros are [28]:

$$\psi_i = 2\cos^{-1}\left(\frac{y_i}{y_0}\right), \quad Z_i = 2\exp[j\psi_i], \tag{23}$$

where $\cos^{-1}(.)$ is the inverse cosine function, $j = \sqrt{-1}$. The z-transform of the array factor, $\mathbf{a}(Z)$, is then [28]:

$$\mathbf{a}(Z) = Z^{-(M-1)/2} \prod_{i=1}^{M-1} (Z - Z_i). \tag{24}$$

The coefficients, $\mathbf{a_c}$ of dimension $1 \times M$, of the inverse z-transform of $\mathbf{a}(Z)$ are the weight vector, which is steered towards ϕ_k to generate the Dolph-Chebyshev steering vector, $\mathbf{a}_d(\phi_k)$ according to, $\mathbf{a}_d(\phi_k) = \mathbf{a_c} \circ \mathbf{a}(\phi_k)$, where $(\circ)$ denotes the Hadamard product, i.e., element-wise multiplication of the two vectors $\mathbf{a_c}$ and $\mathbf{a}(\phi_k)$. Note that for ULA, $\mathbf{a}(\phi_k)$ is defined in (3).

C. SEQUENTIAL VS. BINARY SEARCH

XSBS sequentially scans the angular region of interest, i.e., spatial domain, to collect K directed signals. XSBS then estimates the cross correlation coefficient for the K beams. This sequential search for the highest peak leads to a longer operation time to detect the AoA. In the context of hiding transmitter, the transmitted signal may not be available for a long time. Therefore, quick estimation of the AoA is a key parameter in a efficient AoA system. We propose to use binary search for the peak location rather than sequential, which has two benefits. In binary peak location search, the angular region of interest is divided into two equal regions. The cross correlation coefficient is estimated for the two signals collected from the two regions. The half with the higher cross correlation coefficient is then divided into two equal halves and so on. To do so, the *Weights Unit* adjust the weights accordingly. A subset of the antenna array can be used to achieve this target since lower number of antenna array elements leads to higher HPBW. The rest of the antenna array elements will be switched off using the RF switches. The first benefit of binary search is that it reduces the number of cross correlation estimation from K to $\log_2 K$. For example, for our simulation below with $K = 32$ beams, binary peak search requires the estimation of only 5 beams rather than 32 as in the case of sequential search. The second benefit is that it significantly increases the main lobe to side lobe ratio (R) such that almost no signal is leaked through a side

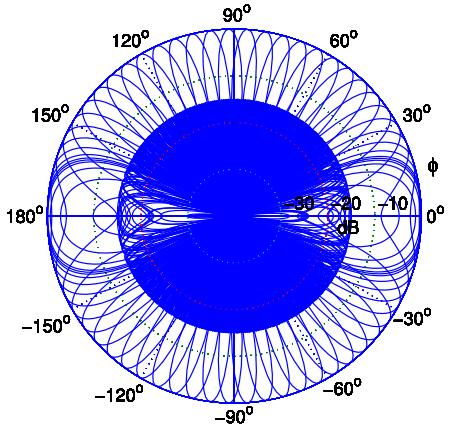

FIGURE 4. Beam switching antenna array for $M = 17$ with Dolph-Chebychev excitation, $R = 15$ dB and $d = 0.5\lambda$ with a total of 32 orthogonal beams with HBPW = 6 degrees.

lobe. We start by high HPBW and then reduce it as we get closer to the target. With high HPBW required, the main lobe to side lobe ratio can be very high.

Indeed, during the first steps of binary search, when using a beam with a wide HPBW, the antenna array gain reduces. However, this can be thought of as a tradeoff between speed (number of scans) and sensitivity. One can get an intuition about that from Phase I. If the signal collected in Phase I is strong, then it is very likely that the performance will not be affected by the gain variation of wider beams.

VI. PERFORMANCE EVALUATION

First we present results for XSBS's angular resolution. We then plot the probability of detection of ED versus the probability of false alarm for different number of samples as well as different SNR levels. XSBS AoA estimation performance is then compared to MUSIC in terms of peak to floor ratio (PFR), root mean square error (RMSE) and 3-dB success rate for single transmitter case. We then compare the spatial resolution and RMSE of XSBS and MUSIC for two transmitters.

A. XSBS PRACTICAL ASPECTS

We start by analyzing the resolution of XSBS; we plot the steered antenna array beam for $M = 17$, separation $d = 0.5\lambda$, $R = 15$ dB, with Dolph-Chebyshev non-uniform excitation in Fig. 4. The achieved HPBW is approximately 6 degrees with a total of $K = 32$ *orthogonal* beams scanning the 180 degrees[2]. As M increases, the resolution of XSBS improves since the HPBW decreases.

B. XSBS SPECTRUM SENSING

We plot the receiver operating characteristic curves (ROC) of ED spectrum sensing when the distributions of the received signal under the two hypotheses are as described earlier.

[2]Fig. 4 is plotted using the MATLAB toolbox of [28].

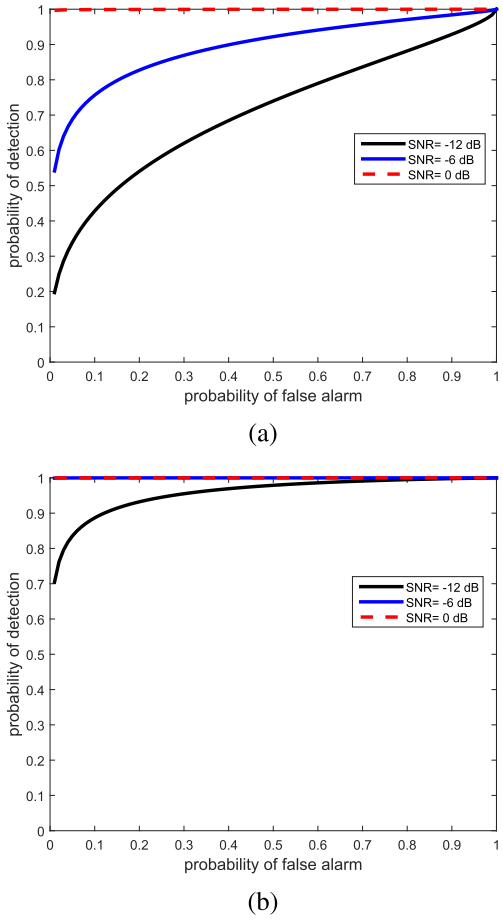

FIGURE 5. ROC curves for ED for different SNR values for (a) $N = 100$ and $N = 1000$ samples.

The ROC curve plots the probability of detection, P_d, versus the probability of false alarm, P_f. A higher probability of detection achieved with lower probability of false alarm is the desired performance. We plot the numerically computed ROC curves in Fig. 5 for different SNR levels and for (a) $N = 100$ and (b) $N = 1000$. As expected, as SNR or N increases, the performance of ED improves. Hence, based on the desired SNR dynamic range, N should be selected to achieve the desired standard performance of $P_d = 90\%$ with $P_f = 10\%$.

C. XSBS AoA ESTIMATION

In the following we evaluate the performance of XSBS AoA estimation with respect to different aspects. We evaluate the performance of XSBS when varying the incident angle. We present the PFR as an intuition that XSBS can correctly estimate the true AoA. We compare RMSE and 3-dB success rate of XSBS. We show how XSBS performs when two sources are impinging on the antenna array.

The simulation settings in the subsequent figures are as follows. We simulate XSBS with linear antenna array with Dolph-Chebyshev excitation using $M = 17$. MUSIC uses uniform linear antenna array with $M = 16$. We plot the normalized cross correlation coefficient (12) to represent the

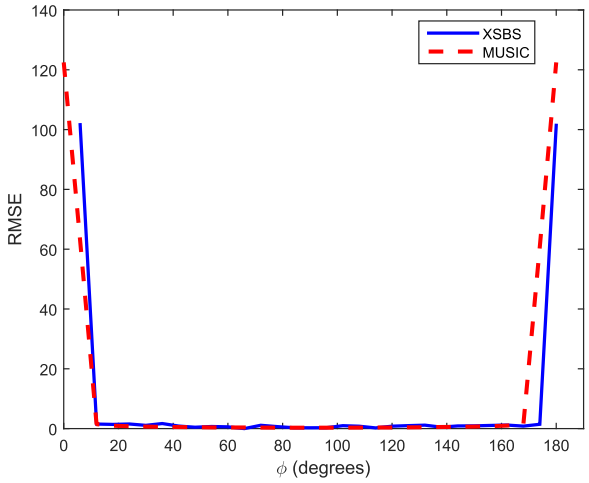

FIGURE 6. RMSE versus incident AoA for $N = 100$ samples at SNR $= -10$ dB. Similar to MUSIC, the performance of XSBS is consistent when varying the incident angle.

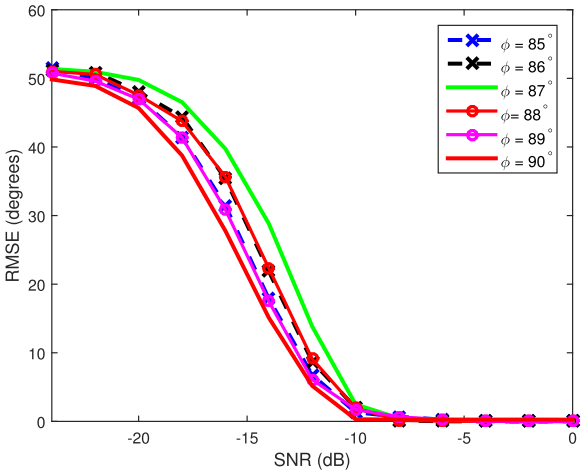

FIGURE 7. RMSE for XSBS versus SNR for $\phi = 85°, 86°, 87°, 88°, 89°$ and $90°$ for $N = 100$ samples. Within the operational SNR range, the performance of XSBS is consistent for all incident angles between peak locations.

spatial power, versus the azimuth angle ϕ. We assume a strong line of sight with block fading (i.e channel is almost constant during the whole processing time). The reference of the incident azimuth angle is the plane containing the linear antenna array. It is worth noting that XSBS can operate with any antenna array formation with known steering vector and is not strictly designed to operate with ULA.

As we stated in the System Model, we can safely assume that the transmitter continues to transmit a highly correlated signal during the scanning time of XSBS. For example, for a number of beams $K = 32$ and if we collect $N = 1000$ samples from each direction and for a sampling frequency of 5 MHz, the total scanning time is 6.4 milliseconds. Moreover, we proposed binary search approach that reduces the number of required scans from K to $\log_2 K$. For the provided example, the number of scans reduces to 5, which reduces our scanning time to 1 millisecond. For a sampling frequency of 20 MHz, the scanning time is further reduced to the quarter, i.e., 250 and 25 microsecond for $N = 1000$ and 100 samples, respectively.

1) RMSE VERSUS INCIDENT ANGLE

In Fig. 6, we plot the RMSE of XSBS and MUSIC for $N = 100$ samples at SNR $= -10$ dB with the incident angle spanning the 180°. This shows that aside from the poor performance towards the sides of the antenna array, which is common behavior between XSBS and MUSIC, the performance of XSBS is consistent regardless of the location of the incident angle. Hence, in the subsequent figures, we could use any arbitrary angle within the operating range (approximately 15° to 165°) and the results will be the same.

We show an example of the performance of XSBS versus SNR for all incident angles between two orthogonal beams. In other words, all angles between two beam peaks. We select two beams with peaks located at 84° and 90°. In Fig. 7, we plot the RMSE for XSBS when the transmitter signal is impinging at angles 85°, 86°, 87°, 88°, 89° and 90° versus SNR for $N = 100$ samples. The received signal is received by the two adjacent orthogonal beams at 84° and 90°, but with different array gain factor, G_k. As can be seen by comparing the peaks at the two adjacent beams, we can get very comparable performance for any received AoA using weighted average. Within the operational SNR range, i.e., when RMSE is close to zero, the RMSE is almost the same for all angles.

2) PEAK TO FLOOR RATIO

In Fig. 8, we simulate XSBS and MUSIC at SNR $= -10$ dB for $N = 100$, 1000 and 2000 samples for a signal with arriving angle $\phi_k = 90°$ for a single run (top) and an average of 1000 iteration (bottom).

It is shown that XSBS can accurately determine the correct AoA by having the highest peak at the location of the incident angle. Increasing the number of samples improves the performance of XSBS. XSBS achieves PFR $= 8$ dB, 15 dB and 17 dB for $N = 100$, 1000 and 2000 samples, respectively. MUSIC has a higher PFR achieving PFR $= 10$ dB, 18 dB and 22 dB for $N = 100$, 1000 and 2000 samples, respectively.

3) EFFECT OF MAIN LOBE TO SIDE LOBE RATIO

As we stated earlier, the main lobe to side lobe ratio (R) is a design parameter. When using binary search, we start by high HPBW, for which it is possible for R to be very high such that the signal is received through the main lobe only. However, as we get closer to the location of the incident angle, we must reduce the HPBW of the main lobe, which results in signal getting leaked through a side lobe. This mainly occurs during the last cross-correlation estimation step. In Fig. 9, we simulate the scenario of the last binary search step for different values of $R = 15, 25$ and 30 dB. The results are the average of 10000 iterations. The true AoA is 90° and a signal is leaked through a side lobe directed at 108°. Even in the worst case scenario, i.e., $R = 15$ dB, XSBS still can correctly estimate the correct AoA with approximately 8 dB

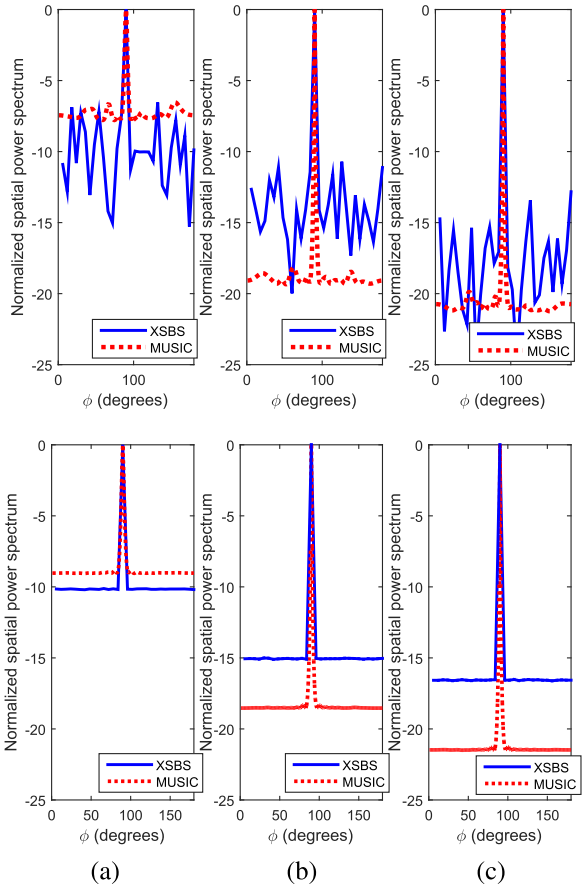

FIGURE 8. PFR for XSBS vs. MUSIC for single run (top) and average of 1000 iterations (bottom) at SNR $= -10$ dB for different number of samples (a) $N = 100$, (b) $N = 1000$ and (c) $N = 2000$ samples. Similar to MUSIC, XSBS has the highest peak at the true AoA with comparable PFR.

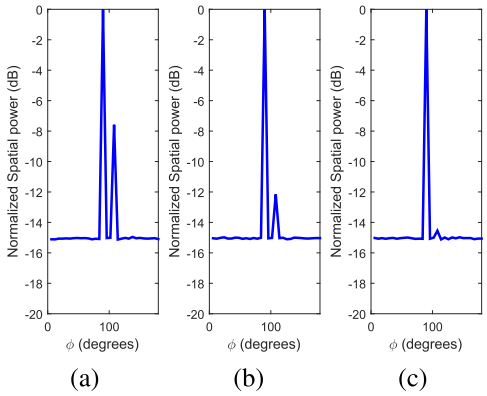

FIGURE 9. Effect of main lobe to side lobe ratio on the performance of XSBS for $N = 1000$ samples at SNR $= -10$ dB (a)$R = 15$ dB, (b) $R = 25$ dB and (c)$R = 30$ dB. With appropriately selecting the main lobe to side lobe ratio, it is possible to get rid off the side lobe effect.

difference between the correct peak and the peak caused due to the side lobe issue.

4) PERFORMANCE FOR A SINGLE TRANSMITTER

Fig. 10 depicts the RMSE of XSBS and MUSIC versus SNR (in steps of 2 dB) for different number of samples. XSBS achieves a comparable RMSE to MUSIC with approximately

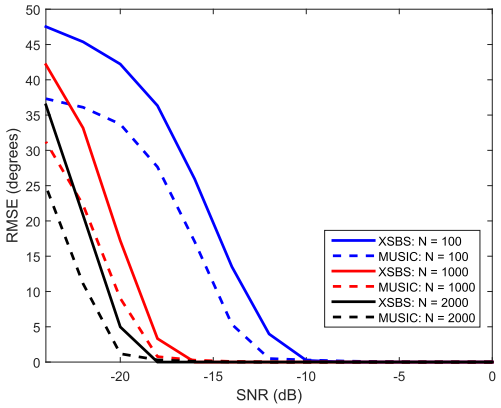

FIGURE 10. RMSE of XSBS and MUSIC vs. SNR for different number of samples for single transmitter. XSBS has comparable performance to MUSIC.

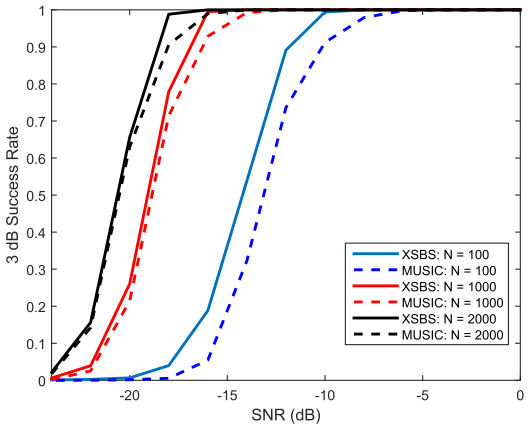

FIGURE 11. 3-dB success rate for XSBS and MUSIC vs. SNR for different number of samples for single transmitter. XSBS has better 3-dB success rate than MUSIC.

2 dB performance gap in favor of MUSIC. For example, for $N = 1000$ samples XSBS requires SNR > -16 dB to achieve RMSE of approximately zero, while MUSIC requires SNR > -18.

Fig. 11 presents the 3-dB success rate versus SNR for XSBS and MUSIC for different number of samples. The 3-dB success rate is defined as the rate at which the estimated angle is the correct angle with the difference between the first peak (success) and the following peak (false) is at least 3 dB. The 3-dB difference between the correct peak and the false peak ensures that the AoA estimation process can be performed efficiently with lower probability of error. On the contrary of the RMSE, XSBS outperforms MUSIC with respect to the 3-dB success rate. This indicates that if the threshold is set at 3-dB level, XSBS will have lower probability of error than MUSIC.

5) PERFORMANCE FOR TWO TRANSMITTERS

We evaluate the performance of XSBS versus MUSIC when two signals are impinging on the antenna array. The two sources for MUSIC are uncorrelated while we use

TABLE 1. Comparison between MUSIC and XSBS.

Item	MUSIC	XSBS
Number of receivers	M, where M is the number of antennas	1
EVD	Yes	No
Number of sources	Must be known a priori	Not needed
Correlation between sources	should be uncorrelated	Works for both correlated and uncorrelated
Maximum number of sources	$M-1$	K, where K is the number of generated beams
Computational Complexity	$\mathcal{O}\left(M^2N+M^3+JM\right)$	$\mathcal{O}\left(MN\right)$

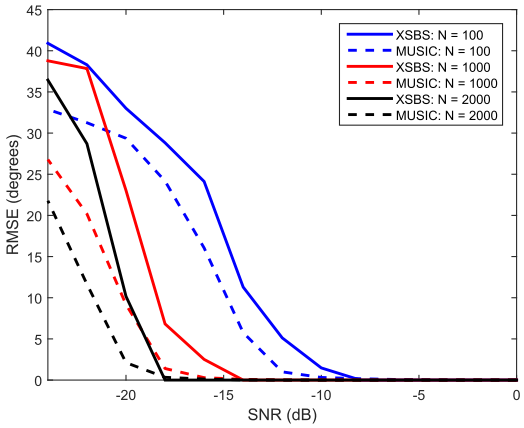

FIGURE 12. RMSE of XSBS vs. MUSIC for two sources at angles $\phi_1 = 90°$ and $\phi_2 = 114°$ against SNR using different number of samples.

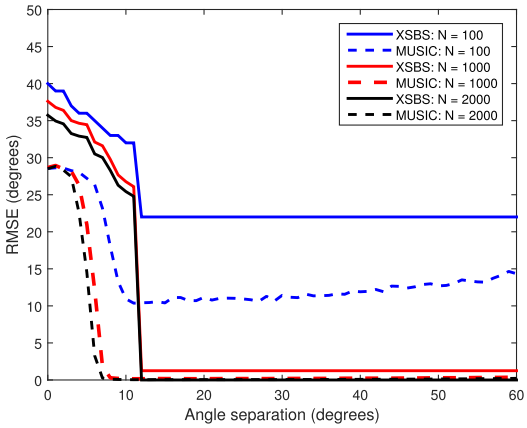

FIGURE 13. Resolution of MUSIC vs. XSBS for different number of samples at SNR = −15 dB. Resolution of XSBS depends mainly on the HPBW.

un-coherent signals for the two sources for XSBS. In Fig. 12, we plot the RMSE for XSBS and MUSIC for two sources versus SNR for different number of samples. The degradation in performance for MUSIC and XSBS due to the second source is approximately 2 dB.

In Fig. 13, we compare the multi-source resolution of XSBS to the multi-source resolution of MUSIC. It is shown that the resolution of MUSIC highly depends on the received SNR and number of samples while for XSBS, it depends mainly on the HPBW of the main lobe, which is determined based on the number of antenna elements M and the type of excitation. For example for $N = 1000$ samples, the resolution of MUSIC is about 8°, while the resolution of XSBS is 12°.

VII. COMPLEXITY COMPARISON

Complexity analysis provides a qualitative measure of system power consumption as well as real-time processing abilities both on software and hardware subsystems which are critical in dynamic environment such as battlefield. Although MUSIC has slightly better performance than XSBS, XSBS uses a single RF receiver chain, which is a tremendous reduction in hardware complexity as well as power consumption. In addition, the computational complexity analysis below show that XSBS uses negligible number of computations when compared to MUSIC that has high computational complexity.

For MUSIC, there are three major computational steps needed to estimate the AoA. The first one is the autocovariance function, which requires multiplication of two matrices with sizes $M \times N$ and $N \times M$. The exact number of floating-point operations (flops) needed for this matrix multiplication is $M^2(2N-1)$. The complexity of the first step is $\mathcal{O}\left(M^2N\right)$. The second step is the EVD operation, which has a complexity of $\mathcal{O}\left(M^3\right)$ [33]. The third step is obtaining the spatial pseudo-spectrum, which has a complexity of $\mathcal{O}\left(JM\right)$ [30], with J being the number of spectral points of the total angular field of view. Therefore, the complexity of MUSIC is given by $\mathcal{O}\left(M^2N+M^3+JM\right)$. In [33], the complexity of MUSIC is given by $\mathcal{O}\left(M^2N+M^2L\right)$, with L being the number of potential AoAs. In [34], the EVD is simplified using the fast decomposition technique [35], which reduces the complexity of MUSIC to $\mathcal{O}\left(M^2L+M(M-L)J+(M-L)J\right)$. Furthermore, the computational complexity for ESPRIT is $\mathcal{O}\left(M^2N+M^3\right)$ [36].

For XSBS, (12) is applied on two vectors each has a dimension of $1 \times N$. The vector multiplication in (12) for each $k \in [1:K]$ requires N multiplications and $N-1$ additions. Therefore, for K beams, the exact number of flops is $K(2N-1)$. Hence, the complexity of XSBS is $\mathcal{O}\left(KN\right)$. For non uniform excitation, $K \approx 2M$, which reduces the complexity to $\mathcal{O}\left(MN\right)$. Consequently, the computational complexity of XSBS is considerably less than the complexity needed in the first step of MUSIC only.

In Table 1, we present a comparison between XSBS AoA estimation and MUSIC in terms of different criteria. It is clear that XSBS has lower hardware and computational complexities and less stringent requirements than MUSIC.

VIII. CONCLUSION

We proposed a hardware friendly AoA estimation system to detect the AoA. Our system can operate with any antenna array formation with known steering vector. We showed that our system can operate at low SNR levels. The number of sources that can be detected using our system is limited by the number of switched beams, which is greater than or equal to the number of antenna elements. We compared our system to MUSIC algorithm and show that our algorithm has a comparable performance. Unlike MUSIC, our system requires a single receiver, which reduces the hardware complexity tremendously. Moreover, our system is based on estimating the cross correlation coefficient between one dimensional vectors, which has a negligible computational complexity. Hence, the practicality and simplicity of our system. In other words, we sacrifice a little bit of performance, but on the favor of huge savings on hardware and computational complexities. The lower hardware and computational complexities lead to a less consumed power than conventional techniques. Hence, it can be used to search for the angle of transmitters, that transmit at random times. In addition, less required power makes the system more portable than existing ones. XSBS requires SNR > -10, -16 and -18 dB for $N =$, 100, 1000 and 2000 samples, respectively to achieve a negligible RMSE.

REFERENCES

[1] B. Liao, Z. Zhang, and S. Chan, "A new robust Kalman filter-based subspace tracking algorithm in an impulsive noise environment," *IEEE Trans. Circuits Syst. II, Express Briefs*, vol. 57, no. 9, pp. 740–744, Sep. 2010.

[2] A. Badawy, T. Khattab, T. Elfouly, D. Mohamed, A. Trinchero, and C. Chiasserini, "Secret key generation based on AOA estimation for low SNR conditions," in *Proc. IEEE 81st Veh. Technol. Conf. (VTC Spring)*, May 2015, pp. 1–7.

[3] T. E. Tuncer and B. Friedlander, *Classical and Modern Direction-of-Arrival Estimation*. San Diego, CA, USA: Academic, 2009.

[4] C. A. Balanis and P. I. Ioannides, "Introduction to smart antennas," *Synthesis Lect. Antennas*, vol. 2, no. 1, pp. 1–175, 2007.

[5] Z. Chen, G. Gokeda, and Y. Yu, *Introduction to Direction-of-Arrival Estimation*. Norwood, MA, USA: Artech House, 2010.

[6] S. Chandran, *Advances in Direction-of-Arrival Estimation*. Norwood, MA, USA: Artech House, 2006.

[7] J. Foutz, A. Spanias, and M. K. Banavar, *Narrowband Direction Arrival Estimation for Antenna Arrays*. San Rafael, CA, USA: Morgan & Claypool, 2006.

[8] M. S. Bartlett, "Periodogram analysis and continuous spectra," *Biometrika*, vol. 37, nos. 1–2, pp. 1–16, 1950. [Online]. Available: http://biomet.oxfordjournals.org/content/37/1-2/1.short

[9] J. Capon, "High-resolution frequency-wavenumber spectrum analysis," *Proc. IEEE*, vol. 57, no. 8, pp. 1408–1418, Aug. 1969.

[10] R. O. Schmidt, "A signal subspace approach to multiple emitter location and spectral estimation," Ph.D. dissertation, Dept. Elect. Eng., Stanford Univ., Stanford, CA, USA, 1981.

[11] P. Stoica, P. Handel, and A. Nehoral, "Improved sequential MUSIC," *IEEE Trans. Aerosp. Electron. Syst.*, vol. 31, no. 4, pp. 1230–1239, Oct. 1995.

[12] A. J. Weiss and B. Friedlander, "DOA and steering vector estimation using a partially calibrated array," *IEEE Trans. Aerosp. Electron. Syst.*, vol. 32, no. 3, pp. 1047–1057, Jul. 1996.

[13] R. Roy and T. Kailath, "Esprit-estimation of signal parameters via rotational invariance techniques," *IEEE Trans. Acoust., Speech, Signal Process.*, vol. 37, no. 7, pp. 984–995, Jul. 1989.

[14] H. H. Chen, S. C. Chan, Z. G. Zhang, and K. L. Ho, "Adaptive beamforming and recursive DOA estimation using frequency-invariant uniform concentric spherical arrays," *IEEE Trans. Circuits Syst. I, Reg. Papers*, vol. 55, no. 10, pp. 3077–3089, Nov. 2008.

[15] X. Zhang and D. Xu, "Low-complexity ESPRIT-based DoA estimation for colocated MIMO radar using reduced-dimension transformation," *Electron. Lett.*, vol. 47, no. 4, pp. 283–284, Feb. 2011.

[16] Z. Tan, Y. C. Eldar, and A. Nehorai, "Direction of arrival estimation using co-prime arrays: A super resolution viewpoint," *IEEE Trans. Signal Process.*, vol. 62, no. 21, pp. 5565–5576, Nov. 2014.

[17] Q. Shen, W. Liu, W. Cui, S. Wu, Y. Zhang, and M. Amin, "Low-complexity direction-of-arrival estimation based on wideband co-prime arrays," *IEEE/ACM Trans. Audio, Speech, Language Process.*, vol. 23, no. 9, pp. 1445–1456, Sep. 2015.

[18] J.-F. Gu, S. C. Chan, W.-P. Zhu, and M. N. S. Swamy, "Joint DOA estimation and source signal tracking with Kalman filtering and regularized QRD RLS algorithm," *IEEE Trans. Circuits Syst. II, Express Briefs*, vol. 60, no. 1, pp. 46–50, Jan. 2013.

[19] K. A. Gotsis, K. Siakavara, and J. N. Sahalos, "On the direction of arrival (DoA) Estimation for a switched-beam antenna system using neural networks," *IEEE Trans. Antennas Propag.*, vol. 57, no. 5, pp. 1399–1411, May 2009.

[20] Y. Ozaki, J. Ozawa, E. Taillefer, J. Cheng, and Y. Watanabe, "Direction-of-arrival estimation using adjacent pattern power ratio with switched beam antenna," in *Proc. IEEE Pacific Rim Conf. Commun., Comput. Signal Process. (PacRim)*, Aug. 2009, pp. 453–458.

[21] J. Lee, D. Kim, C. K. Toh, T. Kwon, and Y. Choi, "A table-driven AOA estimation algorithm for switched-beam antennas in wireless networks," in *Proc. 11th Eur. Wireless Conf. Next Generation Wireless Mobile Commun. Services (Eur. Wireless)*, Apr. 2005, pp. 1–6.

[22] J. Werner, J. Wang, A. Hakkarainen, D. Cabric, and M. Valkama, "Performance and CramerŰRao bounds for DoA/RSS estimation and transmitter localization using sectorized antennas," *IEEE Trans. Veh. Technol.*, vol. 65, no. 5, pp. 3255–3270, May 2016.

[23] M. Ringer and G. J. Frazer, "Waveform analysis of transmissions of opportunity for passive radar," in *Proc. 15th Int. Symp. Signal Process. Appl. (ISSPA)*, vol. 2. Jan. 1999, pp. 511–514.

[24] C. Berger, B. Demissie, J. Heckenbach, P. Willett, and S. Zhou, "Signal processing for passive radar using ofdm waveforms," *IEEE J. Sel. Topics Signal Process.*, vol. 4, no. 1, pp. 226–238, Feb. 2010.

[25] C.-C. Chen and W. A. Gardner, "Signal-selective time-difference of arrival estimation for passive location of man-made signal sources in highly corruptive environments. II. Algorithms and performance," *IEEE Trans. Signal Process.*, vol. 40, no. 5, pp. 1185–1197, May 1992.

[26] H. Yan and W. Liu, "Design of time difference of arrival estimation system based on fast cross correlation," in *Proc. 2nd Int. Conf. Future Comput. Commun. (ICFCC)*, vol. 2. May 2010, pp. V2-464–V2-466.

[27] P. Peng, H. Luo, Z. Liu, and X. Ren, "A cooperative target location algorithm based on time difference of arrival in wireless senor networks," in *Proc. Int. Conf. Mechatronics Autom. (ICMA)*, Aug. 2009, pp. 696–701.

[28] S. J. Orfanidis. (2010). *Electromagnetic Waves and Antennas*. [Online]. Available: http://www.ece.rutgers.edu/ orfanidi/ewa/

[29] H. Krim and M. Viberg, "Two decades of array signal processing research: The parametric approach," *IEEE Signal Process. Mag.*, vol. 13, no. 4, pp. 67–94, Jul. 1996.

[30] A. Khallaayoun, "A high resolution direction of arrival estimation analysis and implementation in a smart antenna system," Ph.D. dissertation, Dept. Elect. & Comput. Eng., Montana State University, Bozeman, MT, USA, 2010.

[31] H. Urkowitz, "Energy detection of unknown deterministic signals," *Proc. IEEE*, vol. 55, no. 4, pp. 523–531, Apr. 1967.

[32] F. F. Digham, M.-S. Alouini, and M. K. Simon, "On the energy detection of unknown signals over fading channels," *IEEE Trans. Commun.*, vol. 55, no. 1, pp. 21–24, Jan. 2007.

[33] C. Stoeckle, J. Munir, A. Mezghani, and J. A. Nossek, "DoA estimation performance and computational complexity of subspace- and compressed sensing-based methods," in *Proc. 19th Int. ITG Workshop Smart Antennas*, Mar. 2015, pp. 1–6.

[34] Y. Zhang and B. P. Ng, "MUSIC-like DOA estimation without estimating the number of sources," *IEEE Trans. Signal Process.*, vol. 58, no. 3, pp. 1668–1676, Mar. 2010.

[35] G. Xu and T. Kailath, "Fast subspace decomposition," *IEEE Trans. Signal Process.*, vol. 42, no. 3, pp. 539–551, Mar. 1994.

[36] C. Qian, L. Huang, and H. C. So, "Computationally efficient ESPRIT algorithm for direction-of-arrival estimation based on Nyström method, " *Signal Process.*, vol. 94, pp. 74–80, Jun. 2014.

AHMED BADAWY (S'15) received the bachelor's degree in electrical engineering from the University of Nevada, Reno, USA, in 2008, and the M.Sc. degree from Montana State University, Bozeman, USA, in 2010. He is currently pursuing the Ph.D. degree with the Department of Electronics and Telecommunications, Politecnico di Torino, Italy. His research interests include cognitive radios, physical layer security, smart antenna systems, and hardware implementation of communication systems.

TAMER KHATTAB (M'94) received the B.Sc. degree in electronics and communications engineering from Cairo University, Giza, Egypt, the M.Sc. degree in electronics and communications engineering, and the Ph.D. degree in electrical and computer engineering from the University of British Columbia, Vancouver, BC, Canada, in 2007. From 2006 to 2007, he was a Post-Doctoral Fellow with the University of British Columbia, where he was involved in prototyping advanced gigabit/sec wireless LAN baseband transceivers. From 2000 to 2003, he joined Alcatel Canada's Network and Service Management Research and Development, Vancouver, as a member of the Technical Staff, where he was involved in the development of core components for Alcatel 5620 network and service manager. From 1994 to 1999, he was with IBM wtc. Egypt as a software development team lead working on development of several client-server corporate tools for IBM labs. He has been an Assistant Professor of Electrical Engineering with Qatar University (QU) since 2007. He is currently a Senior Member of the Technical Staff with the Qatar Mobility Innovation Center (QMIC), an Research and Development center owned by QU and funded by Qatar Science and Technology Park. His research interests cover physical layer transmission techniques in optical and wireless networks, information theoretic aspects of communication systems, and MAC layer protocol design and analysis.

DANIELE TRINCHERO (S'94–M'08) was born in Turin, Italy, in 1968. He received the Laurea degree in electronic engineering and the Ph.D. degree in electronic and telecommunication engineering from the Politecnico di Torino, Turin, in 1993 and 1997, respectively. He was with the Italian National Council of Research, Turin. In 1996, he visited Loughborough University, Loughborough, U.K. Since 1997, he has been with the Electronics Department, Politecnico di Torino, where he founded iXem Labs, in 2005, and since 2005, he has been responsible for them. He is also affiliated with the Institute of Electronics and Information and Telecommunication Engineering, CNR. With the Politecnico di Torino, he teaches courses on basic electromagnetic theory, radio planning, electromagnetic compatibility, and electromagnetic field measurements.

He is a Reviewer of several international publications. His major field of study is related to electromagnetic field propagation applied to the design of wireless components and networks.

His research interests include wireless sensor networks, geographical wireless networks, long-distance communications, antennas, electromagnetic field propagation, electromagnetic field measurements, electromagnetic compatibility, microwave devices, frequency-selective surfaces, shielding devices, and wireless solutions for digital inclusion of developing regions.

TAREK M. ELFOULY (M'06–SM'13) received the DEA and Ph.D. degrees from the University of Franche Comte, France, in 1996 and 2000, respectively. He was an Assistant Professor with the University of Ain Shams, Cairo, Egypt. He is currently an Assistant Professor with the College of Engineering, Qatar University.

He has over ten years of experience in computer network research. He has authored over 40 papers, over half of them are related to wireless sensing and network security.

Dr. Elfouly has many projects under development related to assistive technologies for people with disabilities. His projects won many national and regional awards.

His research interests include network security and protocols, physical layer security, and wireless sensor networks, especially in the field of structural health monitoring and health applications.

AMR MOHAMED (S'00–M'06–SM'14) received the M.S. and Ph.D. degrees in electrical and computer engineering from the University of British Columbia, Vancouver, Canada, in 2001 and 2006, respectively. He was an advisory IT Specialist with the IBM Innovation Centre, Vancouver, from 1998 to 2007, taking a leadership role in systems development for vertical industries. He is currently an Associate Professor with the College of Engineering, Qatar University, and also the Director of the Cisco Regional Academy.

He has over 20 years of experience in wireless networking research and industrial systems development. He holds three awards from IBM Canada for his achievements and leadership, and three best paper awards.

His research interests include networking and MAC layer techniques mainly in wireless networks. He has authored or co-authored over 80 refereed journal and conference papers and one textbook.